Mon. Not. R. astr. Soc., (1981) **197**, 413–428

A search for the infrared counterpart of type II OH masers – I. A model for the IR background source confusion

Terry J. Jones, Michael Ashley, A. R. Hyland and A. Ruelas-Mayorga *Mount Stromlo and Siding Spring Observatories, Research School of Physical Sciences, Australian National University, Private Bag, Woden PO, ACT 2606, Australia*

Received 1981 February 2

Summary. A simple exponential disc model for the distribution of stars and extinction (dust) in the galaxy is developed for the purpose of predicting the infrared stellar luminosity function along an arbitrary line of sight at any given wavelength and apparent magnitude limit. The model luminosity function is used to determine the extent to which the stellar field will contaminate searches for the infrared counterpart of type II OH masers. The model parameters are calibrated using 2.2 μm source count data available in the literature, and new data presented here for the first time. In the plane, contamination by the field is found to be serious by 8th magnitude at 2.2 μm and 7th magnitude at 3.5 μm for a 20 arcsec radius search area.

1 Introduction

Celestial sources which exhibit double peaked 1612 MHz OH emission have long been associated with stars that are bright infrared sources (Wilson & Barrett 1972: Wilson, Barrett & Moran 1970; Hyland *et al.* 1972). Originally, radio telescopes were pointed at the coordinates of known infrared objects to check for OH emission. If 1612 MHz emission was found, then the identification of the OH source with the IR object was fairly secure, since double peaked OH sources are quite rare. More recently, the reverse procedure has been used. With extensive surveys of the galactic plane at 1612 MHz (Caswell *et al.* 1981; Baud 1978; Winnberg *et al.* 1975; Caswell & Haynes 1975), many new OH masers with the characteristic type II OH/IR spectral features have been discovered. Subsequently, several authors (Evans & Beckwith 1977; Schultz, Kreysa & Sherwood 1976; Glass 1978) have searched at these positions at IR wavelengths for the expected IR stellar counterpart. Only in the case of Evans & Beckwith were the radio positions of comparable accuracy to the pointing and beam sizes of optical telescopes (a few arcsec). Generally the radio positions are much less accurate (± 15 to ± 30 arcsec) and larger areas of the sky must be searched in order to make a secure identification of the infrared counterpart. At this point a fundamental question

arises. To what extent does the background field in the galactic plane influence the plausibility of the identification of a stellar infrared source with a radio object? There are two basic factors which influence this question.

1. The area searched. Clearly, the larger the area on the sky that must be searched, the greater the probability of finding a field star at any given apparent magnitude, bearing in mind that in the galactic plane at IR wavelengths the background field is composed of a very different set of stars than the field visible on optical photographs (Elias 1978a; Jones *et al.* 1980). This is due to a combination of lower interstellar extinction and the fact that late-type giants are very bright in the IR.

2. The apparent magnitude of the IR candidate: the brighter the candidate source, the lower the probability that it will be a field star. Furthermore, IR searches cannot be made to arbitrarily faint levels because eventually a field star will be found. Although the discovery of a bright candidate does not ensure that the identification is correct, it does lower the probability that the candidate is a random field star.

There are other criteria that can be applied in an effort to make an identification more secure. For instance, finding that the brightness of an IR candidate varies in step with variations in the OH emission will make an identification virtually certain. Unfortunately such observations require a considerable time base and close collaboration with radio observations, and do not lend themselves to the 'one look' infrared search being considered here. The only other potential information available in a survey other than the position and apparent magnitude of the IR candidate is its colours. Although most identified OH/IR stars show an infrared excess (that is, they lie well off the interstellar reddening line) there is no *a priori* basis for assuming that OH/IR sources found in a radio survey will do the same, at least at near infrared wavelengths (1–4 μm). IR spectra may be useful in separating out any carbon stars (Frogel & Hyland 1972) which, as a class, are probably not OH masers (Hyland *et al.* 1972).

Obviously there would be no problem if all of the OH masers discovered in radio surveys were found to have very bright counterparts in the IR. Unfortunately this has not been the case. Fully half of the radio sources searched for by Schultz *et al.* (1976) were below their detection limit of +5.0 at 3.8 μm (L'). Although Glass (1978) found candidates at 2.2 μm (K) for 14 of the 15 radio sources he searched for, well over half of the candidates were further than 1 σ away from the radio positions (Caswell & Haynes 1975) and several were fainter than 8th magnitude at K. In a subsequent paper we will present data for an IR search for OH/IR stars down to $K = +11$ and $L' = +9$. It is important to find out to what extent the field confuses source identification at these faint levels. Clearly a means of making a reasonably accurate estimate of the field luminosity function at IR wavelengths would be very useful in answering this question. In this paper we develop a simple model of the stellar distribution in the galaxy for use in estimating the probability of associating a field star with an OH source. This model is then calibrated by source count and total flux data available in the literature, and by new data presented here for the first time.

2 Observations

The observations were made on the Stromlo 1.9-m telescope with the MSO IR photometer. Four separate regions were scanned at a sidereal rate through the K (2.2 μm) filter and a 2 mm (12 arcsec) aperture. With the exception of the Coal Sack (Jones *et al.* 1980) all of the source count data in the literature (see Fig. 2) are for directions at least 5° out of the plane, and generally well away from the Galactic Centre. For this reason, we have chosen areas directly in the plane within 50° longitude of the Galactic Centre. The source counts in these

Table 1. Source counts at 2.2 μm.

l (deg)	b (deg)	Area (arcmin^2)	m	N (obs)	log N (corr. deg^{-2})
20	0	69.6	8.5	39	3.30
			9.0	54	3.45
			9.5	75	3.59
			10.0	114	3.79
			10.5	145	3.91
350	0	59.8	8.5	35	3.32
			9.0	61	3.56
			9.5	93	3.77
			10.0	136	3.94
			10.5	167	4.06
340	0	64.4	8.5	21	3.07
			9.0	37	3.32
			9.5	56	3.50
			10.0	84	3.69
			10.5	114	3.83
320	0	51.7	8.5	25	3.24
			9.0	33	3.36
			9.5	54	3.58
			10.0	80	3.77
			10.5	112	3.92

directions are much more sensitive to the basic parameters of any model of the stellar distribution of the galaxy.

A spacing of 6 arcsec in declination between the individual scans was used to ensure complete coverage on the sky. Although the 3 σ level on a strip chart was slightly fainter than $K = +10.5$, the high spatial density of sources fainter than this magnitude made $K = +10.5$ the useful limit for source counts. It was still necessary to correct the fainter magnitudes for overlap. Typically, the corrections were 10–15 per cent for the faintest intervals. The results of these scans are presented in Table 1, where N(obs) is the observed number of stars brighter than apparent magnitude m and log N(corr) is the log of the corrected number per square degree brighter than magnitude m.

3 The model

The model developed here is very similar to the model for source counts at 2.2 μm developed by Elias (1978a). The galaxy is modelled as a pure exponential disc where the number of stars per kpc^3 drops off in an exponential manner radially from the Galactic Centre and perpendicularly to the galactic plane as follows:

$$N_i(r,Z,M) = N_i^* \exp\left(\frac{R-r}{\alpha_r} - \frac{Z}{\beta_Z} - \frac{M-M_i}{2\sigma_i^2}\right) \Big/ (2\pi\sigma_i^2)^{1/2}, \quad (1)$$

where N_i^* is the space number density of stellar type i in the solar neighbourhood. R is the distance of the Sun from the Galactic Centre, taken to be 8.7 kpc (Graham 1979). The spatial variable r is referred to the Galactic Centre and Z to the galactic plane. The variables α_r and β_Z are the exponential scale lengths in the r and Z directions. The use of a Gaussian to approximate the dispersion in intrinsic absolute magnitude about the mean M_i is taken

Table 2. 2.20 μm luminosity function parameters.

Spectral type	M_i	Dispersion	Log (N_i)	β (kpc)
B0, 1	− 3.12	0.5	2.95	0.04
B2, 3	− 1.33	0.5	3.83	0.04
B5	− 0.53	0.5	4.09	0.04
B8-A0	0.34	0.5	5.33	0.07
A2-5	1.33	0.4	5.54	0.10
F-5	1.87	0.5	6.09	0.14
F8-G2 V	3.14	0.3	6.39	0.25
G5 V	3.51	0.3	6.50	0.30
G8-K3 V	4.15	0.5	7.00	0.35
K4-5 V	4.50	0.5	7.05	0.30
M0-1 V	5.00	0.5	7.15	0.30
M2-3 V	5.50	0.5	7.25	0.30
M4-5 V	6.50	1.0	7.35	0.30
F8-G2 III	0.45	1.0	4.65	0.50
G5 III	− 0.08	1.0	4.65	0.50
G8 III	− 0.56	0.8	5.20	0.25
K0, 1 III	− 0.80	0.7	5.59	0.20
K2, 3 III	− 1.66	0.7	5.23	0.20
K4, 5 III	− 3.36	0.6	4.28	0.30
M0 III	− 4.14	0.6	3.48	0.30
M1 III	− 4.40	0.6	3.13	0.30
M2 III	− 4.76	0.6	3.13	0.30
M3 III	− 5.23	0.6	3.13	0.30
M4 III	− 6.04	0.6	3.00	0.30
M5 III	− 6.90	0.5	3.00	0.30
M6 III	− 7.90	0.5	2.45	0.30
M7 III	− 8.90	0.5	2.09	0.30
M8 + III	− 9.90	0.5	1.65	0.30
Young OB	− 4.70	1.2	2.61	0.05
A-G I-II	− 7.00	2.0	1.53	0.05
K-M2 I-II	− 9.50	1.0	1.49	0.05
M3-4 I-II	−11.00	1.0	1.10	0.05

from Elias (1978a). The apparent magnitude at a distance d from the Sun in the direction given by galactic coordinates l and b is

$$m(d,l,b) = M + 10 + 5\log d + A_\lambda(d,l,b). \tag{2}$$

In this case, r and Z are implicit functions of d, l and b. A is the total interstellar extinction along the line of sight l, b to a distance d (in kpc). The absorption in an interval d to $d + \delta d$ is given by

$$\delta A_\lambda(d,l,b) = A_\lambda^* \exp\left(\frac{R-r}{\alpha_A} - \frac{Z}{\beta_A}\right)\delta d, \tag{3}$$

where A_λ^* is the absorption in mag kpc^{-1} in the local solar neighbourhood and once again, r and Z are implicit functions of d, l and b. Note that this formulation of the interstellar extinction does not allow for clumpiness in the distribution of dust in the galaxy, but does allow for variations in extinction with position in the galaxy.

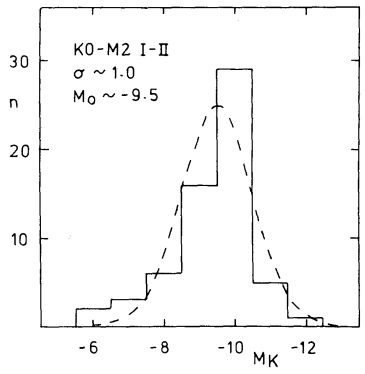

Figure 1. Histogram of the absolute K magnitude distribution for K0–M2 supergiants in the tabulation of Humphreys' (1978). The dotted line is a Gaussian fit to the histogram.

The basic fixed input parameters M_i, N_i^*, β_i and σ_i are listed in Table 2. Most of the values in Table 2 were taken directly from Elias (1978a) except for the addition of late-type dwarfs (Faber *et al.* 1976; Allen 1973) and the stars in young OB associations. Values for young luminous stars were calculated from the tabulated data on luminous stars in the Milky Way by Humphreys (1978). Fig. 1 is a histogram of the absolute K (2.2 μm) magnitude distribution for the K0–M2 supergiants in Humphreys' tabulation and illustrates how M_i and σ_i are obtained. The values of N_i for these luminous stars were obtained by counting the number of each type within 2.5 kpc ($m-M \leqslant 12$) and assuming a scale height in the Z direction of 50 pc. Although young stars contribute a small amount to the star counts, they can contribute a significant fraction of the integrated IR flux in the plane.

The parameters involving the interstellar extinction (A_λ^*, α_A, β_A) were also considered known and fixed. For $A_V^* \sim 1$ mag kpc^{-1} the local extinction at K is $A_K^* \sim 0.07$ mag kpc^{-1}. The scale height in the Z direction is taken to be 0.1 kpc and the radial scale length was fixed at a value that yields the observed reddening in $H-K$ toward the Galactic Centre. This requires a knowledge of the ratio $A_K/E(H-K)$. By taking $E(V-J)/E(B-V) = 2.25$ (Johnson 1968), $E(V-K)/E(B-V) = 2.80$ (Barlow & Cohen 1977; Hackwell & Gehrz 1974), forcing H, L and M to fit the observed colour excess ratios (Jones & Hyland 1980) and extrapolating to $\lambda = \infty$, we obtain $A_K/E(H-K) \sim 1.2$. Becklin *et al.* (1978) derived $E(H-K) = 2.0$ for the Galactic Centre, which implies $A_K \simeq 2.4$. This fixes the scale length for absorption α_A at 4 kpc. For other infrared wavelengths A_λ^* is derived from A_K^* in a manner that satisfies the interstellar reddening curve given by Jones & Hyland (1980).

This leaves the scale length for the stellar distribution α_r as the only free parameter to be adjusted. An empirical value for α_r of 3.7 kpc is derived by de Vaucouleurs (1979) based on the observed optical brightness distribution for $r < R$, which is in fair agreement with the 'scale length' one could associate with the total hydrogen surface density in the interval $0.6\,R < r < R$ (Burton & Gordon 1978). Note that this value is close to the scale length derived for the dust. Unfortunately the observed scale lengths for the surface distribution of gas and stars (optical brightness) in external spiral galaxies are not always the same (Bosma 1978, 1979). Rather, the stellar scale length is shorter. With this in mind, the value for α_r is allowed to vary until a best fit to the available source counts is obtained. The luminosity function for any given l and b is obtained by simply integrating equation (1) in conjunction with equations (2) and (3) in steps of distance along the line of sight l, b.

Fig. 2 illustrates the source count data presently available in the literature. Except for the Coal Sack ($l = 300$, $b = +1$) all of the data are at latitudes of 5° or more out of the plane

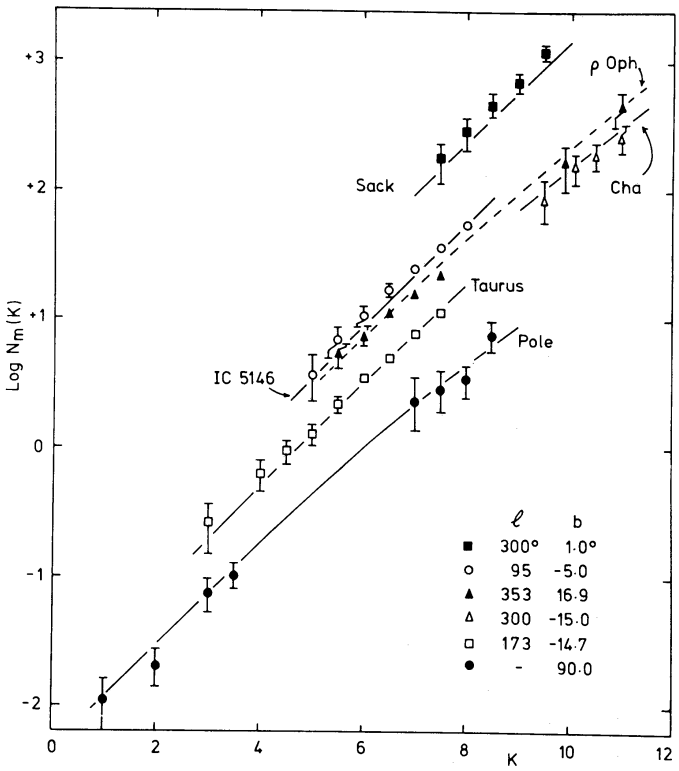

Figure 2. The K filter luminosity function for several areas in the galaxy. The data were taken from the following: Coal Sack, Jones *et al.* (1980); IC5146, Elias (1978a); ρ Oph, Elias (1978b); Chamaeleon, Hyland, Jones & Mitchel (1981); Taurus, Elias (1978c); Pole, Elias (1978d).

and consequently are relatively insensitive to the stellar radial scale length α_r and the interstellar extinction parameters. Thus, this set of source counts principally tests the validity of the local parameters in Table 2. The solid lines in Fig. 2 are the model prediction for α_r = 2.2 kpc (for α_r = 2.5 kpc the results are nearly identical except for the Coal Sack). The excellent fit suggests that the basic input parameters for the solar neighbourhood are not seriously in error. If α_r was made much larger than 3 kpc, however, the model predictions for Taurus, Ophiuchus, and the Coal Sack began to depart significantly from the data.

Fig. 3 illustrates the source count data for $b = 0$ given in Table 1 along with the model predictions for α_r = 2.2 and 2.5 kpc. Only stellar scale lengths shorter than 2.5 kpc could produce model source counts approaching the observations, and α_r = 2.2 kpc gives the best overall fit. This is a rather short scale length, hardly more than half the gas scale length. One could argue that the extinction is modelled incorrectly and that the scale length is actually longer but with much less interstellar extinction. Even if the extinction is held constant at 0.07 mag kpc^{-1} ($\alpha_A = \infty$), the model still requires a relatively short stellar scale length of $\alpha_r \simeq 3$ kpc.

The model can be used to compute the integrated flux (per unit solid angle) at any wavelength by simply summing up the contributions of all magnitude intervals. This procedure is safe at the shorter infrared wavelengths where stellar photospheric radiation is dominant, but could run into problems at longer wavelengths where heated dust in circumstellar shells and H II regions can contribute (e.g. Price & Walker 1976). Broad beam flux measurements of the galactic plane at 2.4μm have been made by several authors (Hayakawa *et al.* 1981; Ito, Matsumoto & Uyama 1977; Okuda *et al.* 1977). Fig. 4 is a synthesis of these observations taken from Hayakawa *et al.* (1981). The solid line is the model prediction for α_r = 2.2 kpc

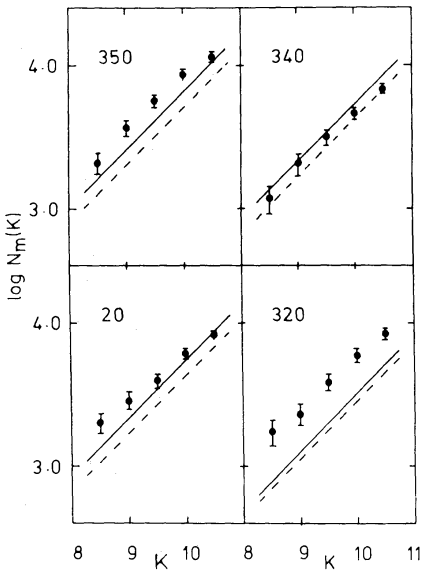

Figure 3. The observed K filter luminosity function for the four directions in the galactic plane listed in Table 1. The solid line is the model prediction for a stellar scale length of α_r = 2.2 kpc; the dotted line is for α_r = 2.5 kpc.

and the dotted line is for α_r = 2.5 kpc. Note that the actual data varies considerably with longitude, but in general lies between the two theoretical curves, except within 5° of the Galactic Centre. Since there is no bulge component in the model, this is not surprising. There is still some controversy over the cause of the peaks and valleys in the 2.4 μm flux distribution in the galactic plane. Okuda (1980) has recently presented observations at 2.2 μm that show an increase in source counts (down to 7th magnitude) at the location of the peaks at $l = 27°$ and $l = 339°$. This discrepancy suggests that there are either more stars along those lines of sight than expected from the old disc, or there is a hole in the extinction, the latter case being the most likely. Such variations in the extinction may explain the discrepancy between the model and the observations at $l = 320$. Note that if the peaks in the flux distribution were due to M supergiants (i.e. enhanced recent star formation) one would expect little, if any, significant increase in star counts down to $K = 7$, since it takes so few M supergiants to influence the integrated flux. The detailed behaviour of the model is discussed in the Appendix.

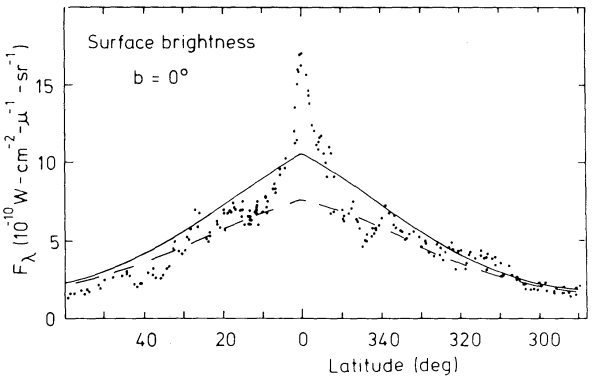

Figure 4. The observed surface brightness the galactic plane at 2.4 μm (Hayakawa *et al.* 1980). The solid line is the model fit for α_r = 2.2 kpc; the dotted line is for α_r = 2.5 kpc.

4 Discussion

The model can now be applied to the IR searches mentioned previously. For Evans & Beckwith (1977), the radio positions are sufficiently precise, and the IR candidates so bright that there is little doubt about the identification. Schultz *et al.* (1976) searched for OH sources from the list of Winnberg *et al.* (1975). They made their search at 3.8 μm and scanned a 1 x 2.2 arcmin box at the radio position of each source. Fourteen of the 29 sources searched for had an IR candidate brighter than the survey limit of 5.0 mag. A histogram of the 3.8 μm magnitude distribution for the 14 candidates is presented in Fig. 5. The solid line represents the model's prediction of the number of stars that would have been found in each magnitude interval for an area of 64 arcmin^2 (29 x 2.2) at $l = 30$, $b = 0$. Since few of the detected IR sources were as far away from the radio position as the edge of the search box, this line represents the least optimistic application of the model. That is to say if two sources of equal brightness were found within a search box, the source closer to the radio position would be chosen. None the less, Fig. 4 clearly shows that at most, only one out of the 14 candidates is likely to be a field star. For a more optimistic approach discussed next, the identifications would be considered almost certain.

Glass (1978) searched for IR counterparts to 15 OH masers from the survey by Caswell & Haynes (1974) at a wavelength of 2.2 μ (K band). He lists 14 candidates brighter than $K = 9$. The K magnitude distribution of these 14 IR sources is plotted in Fig. 7. In this case, we have considered the 'area searched' to be a circular area on the sky with a radius equal to the distance from the radio position to the IR candidates, a very optimistic approach. This area was summed up for all 14 identified sources and used in conjunction with the model predictions for $l = 330$, $b = 0$ to produce the solid line Fig. 6. This result suggests that roughly half of the candidates fainter than 8.0 mag are field stars.

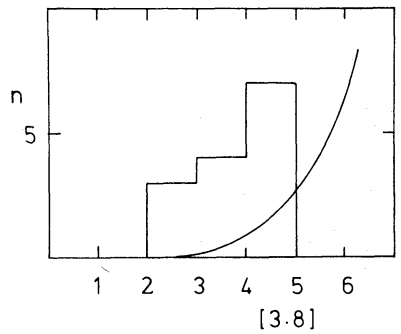

Figure 5. Histogram of the number of OH maser candidates per 3.8 μm magnitude interval found by Schultz *et al.* (1976). The solid line is the model prediction for field stars.

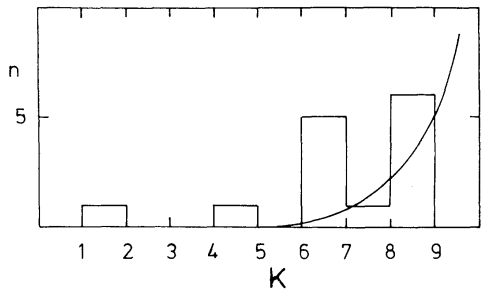

Figure 6. Histogram of the number of OH maser candidates per K magnitude interval found by Glass (1978). The solid line is the model prediction for field stars.

Table 3. Model confusion factor.

Object	Δ (arcsec)	*K*	CF	*P*
327.4 −0.1	1	6.7	0.01	0.01
327.4 −0.6	15	4.3	0.00	0.00
328.2 +0.0	33	8.3	0.26	0.23
328.4 −0.2	8	6.1	0.00	0.00
328.7 −0.2	28	8.0	0.12	0.11
330.4 +0.1	16	8.7	0.09	0.09
331.6 −0.3	28	6.3	0.02	0.02
337.3 −0.2	36	6.4	0.05	0.05
337.4 −0.1	53	7.5	0.37	0.31
337.5 +0.1	49	8.8	1.03	0.64
337.9 +0.3	16	1.5	0.00	0.00
338.0 −0.1	38	8.3	0.40	0.33
338.5 −0.2	40	6.9	0.10	0.10
338.5 +0.1	40	8.6	0.59	0.45

An alternative and better approach would be to compute a confusion factor for each candidate individually. The confusion factor is defined to be the predicted number of field stars in the search area brighter than a given apparent magnitude. This can be done by using the model to compute number of field stars (or fractions thereof) within a solid angle equal to the 'area searched' brighter than the apparent magnitude of the candidate. The distance between the radio and IR positions, or the 1σ error radius on the radio position, whichever is greater, will be used to determine the area searched. This prevents a confusion factor of zero being obtained if the radio and IR positions are by chance very close, even though the probability of the maser source actually being within, say 1 arcsec of the nominal position is very small (for ± 15 arcsec coordinates), and the IR search would obviously not stop at that small a distance anyway.

This procedure has been carried out for the data of Glass and the results are presented in Table 3. The column headed Δ is the distance in arcsec between the IR and radio positions. The column labelled CF (confusion factor) contains the value for the number of field stars within a solid angle $\pi\Delta^2$ or $\pi(15)^2$, brighter than the *K* magnitude in column 3 as predicted by the model at the *l* and *b* of the source. Note that the confusion factor can be greater than one. To convert the confusion factor into the probability *P* of finding at least one field star within the area brighter than the given apparent magnitude, we use the formula

$$P = 1 - \exp(-\mathrm{CF}).$$

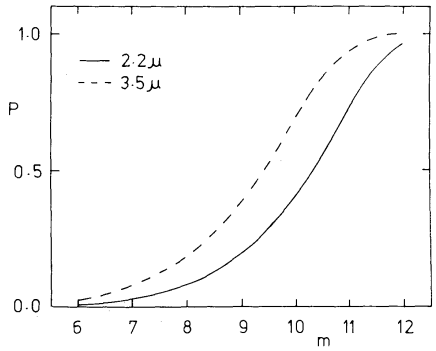

Figure 7. The probability *P* of finding at least one field star brighter than apparent magnitude *m* as a function of *m* for a 20 arcsec radius area at $l = 20$, $b = 0$ computed from the model. Two different wavelengths are shown.

By summing the values in the CF column, an estimate of the number of field stars within the sample can be obtained. This suggests that roughly three out of the 14 candidates are field stars, some having a higher probability of being so than others. Thus, a search at K for OH/IR stars with 15 arcsec radio positions can run into problems of confusion with the field by 8th magnitude. A more general case is illustrated in Fig. 7, which shows the probability P, of finding at least one field star within a 20 arcsec radius disc at $l = 20°$, $b = 0°$. Two wavelengths are illustrated, 2.2 μm (K) and 3.5 μm (L). Note that the curve for L is similar to that for K except it is shifted ~ 1 mag brighter. This is due principally to the reduced interstellar extinction at 3.5 μm, as the $K-L$ colours for late-type giants are only a few tenths at most. For 10.2 μm (N) a similar curve would result except for another shift of ~ 1 mag to the left.

At first glance, Fig. 7 would suggest that K is the better bandpass to search at since a $K-L$ of at least 1 mag is necessary to achieve comparable field confusion at L. As will be shown in the next paper in this series, most of the IR candidates for OH/IR stars do have $K-L$ values of one or greater. More importantly, many candidates are very red, some with a $K-L > 6.0$. These sources could easily be missed at K. The same argument cannot be applied to the N(10.2 μm) band pass however, as compared to L. On the 3-m Infrared Telescope Facility, 9th magnitude at 3.8 μm is easily seen on the strip chart. The reddest OH/IR stars known (e.g., 21.5 + 0.5, 30.1 − 0.7; Evans & Beckwith 1977) have $L-N$ ~ 6 and 3rd magnitude is the practical limit for a 10 μm search using the same rapid scanning that was used at 3.8 μm. Thus, for only the reddest sources does it become marginally better (because of low field confusion) to search at 10 μm, with the potential of missing many bluer sources. Clearly, if one bandpass is to be used in a search for the infrared counterpart of a type II OH maser source, 3.8 μm (L') appears to be the best choice.

5 Conclusion

We have developed a simple but useful model of the stellar distribution in the galaxy that can be used to predict the luminosity function at IR wavelengths at any l and b. This information can then be used to determine the level at which the general stellar field will begin to confuse IR source identifications. The model predictions were then applied to the IR search for OH sources by Schultz *et al.* and Glass (1978). It was found that the field can be a serious problem by 8th magnitude at K and that the 3–4.2 μm atmospheric window is the best bandpass for searches.

References

Allen, C. W., 1973. *Astrophysical Quantities*, 3rd edn, Athlone Press, London.
Baud, B., 1978. *PhD Thesis*, Leiden Observatory.
Barlow, M. J. & Cohen, M., 1977. *Astrophys. J.*, **213**, 737.
Becklin, E. E., Matthews, K., Neugebauer, G. & Willner, S. P., 1978. *Astrophys. J.*, **220**, 831.
Bosma, A., 1978. *PhD Thesis*, University of Groningen.
Bosma, A., 1979. *Astr. Astrophys.*, **79**, 281.
Burton, W. B. & Gordon, M. A., 1978. *Astr. Astrophys.*, **63**, 7.
Caswell, J. L. & Haynes, R., 1975. *Mon. Not. R. astr. Soc.*, **173**, 649.
Caswell, J. L., Haynes, R. F., Goss, W. M. & Mebold, U., 1981. *Aust. J. Phys.*, in press.
de Vaucouleurs, G., 1979. *Observatory*, **99**, 128.
Elias, J. H., 1978a. *Astrophys. J.*, **223**, 859.
Elias, J. H., 1978b. *Astrophys. J.*, **224**, 453.
Elias, J. H., 1978c. *Astrophys. J.*, **224**, 857.

Elias, J. H., 1978d. *Astr. J.*, **83**, 791.
Evans, N. J. & Beckwith, S., 1977. *Astrophys. J.*, **217**, 729.
Faber, S. M., Burstein, D., Tinsley, B. M. & King, I. R., 1976. *Astr. J.*, **81**, 45.
Frogel, J. A. & Hyland, A. R., 1972. *Mem. Soc. R. Sci. Liege, 6th Ser.*, **3**, 111.
Glass, I. S., 1978. *Mon. Not. R. astr. Soc.*, **182**, 93.
Graham, J. A., 1979. *IAU Symp. No. 84*, 195.
Hackwell, J. A. & Gehrz, R. D., 1974. *Astrophys. J.*, **194**, 49.
Hayakawa, S., Matsumoto, T., Murakami, H., Ugama, K., Thomas, J. A. & Yamagami, T., 1981. Preprint.
Humphreys, R. M., 1978. *Astrophys. J. Suppl.*, **38**, 309.
Hyland, A. R., Jones, T. J. & Mitchel, R., 1981. In preparation.
Hyland, A. R., Becklin, E. E., Frogel, J. A. & Neugebauer, G., 1972. *Astr. Astrophys.*, **16**, 204.
Ito, K., Matsumoto, T. & Uyama, K., 1977. *Nature*, **265**, 517.
Johnson, H. L., 1968. *Nebula and Interstellar Matter*, p. 167, University of Chicago Press.
Jones, T. J. & Hyland, A. R., 1980. *Mon. Not. R. astr. Soc.*, **192**, 359.
Jones, T. J., Hyland, A. R., Robinson, G. & Thomas, J. A., 1980. *Astrophys. J.*, **242**, 132.
Okuda, H., 1980. *IAU Symp. No. 96*, eds Wynn-Williams, C. G. & Cruikshank, D. P.
Okuda, H., Maihara, T., Oda, N. & Sugiyama, T., 1977. *Nature*, **265**, 515.
Price, S. D. & Walker, R. G., 1976. *The AFGL Four Colour Sky Survey*. AFGL-TR-76-0208.
Schultz, G. V., Kreysa, E. & Sherwood, W. A., 1976. *Astr. Astrophys.*, **50**, 171.
Wilson, W. J. & Barrett, A. H., 1972. *Astr. Astrophys.*, **17**, 385.
Wilson, W. J., Barrett, A. H. & Moran, J. W., 1970. *Astrophys. J.*, **160**, 545.
Winnberg, A., Nguyen-Q, Rieu, Johansson, L. E. B. & Goss, W. M., 1975. *Astr. Astrophys.*, **38**, 145.

Appendix

The general characteristics of the luminosity function model are described in this section. The model is completely symmetric about the Galactic Centre and the plane. Although this is not likely to be the case in detail for the Milky Way, especially in the case of the interstellar extinction, the present limited data do not justify introducing extra parameters. Indeed, a perfect fit could be achieved by having as many parameters as there are directions with source counts, an absurd situation. Thus the model was formulated with a minimum of parameters, and with the exception of the stellar scale length, they are at least partially, if not wholly, constrained by other observational data.

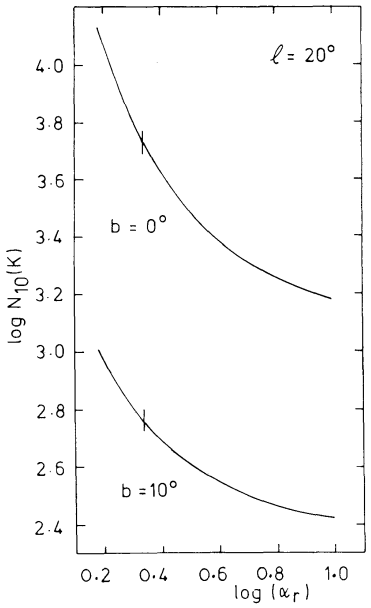

Figure A1. The log of the number of stars brighter than $K = 10$ as a function of the model parameter α_r for $l = 20°$. Two different latitudes are shown.

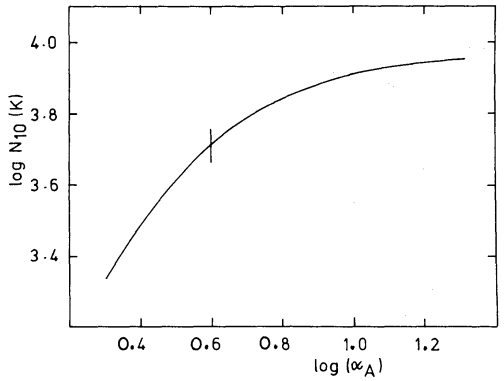

Figure A2. The log of the number of stars brighter than $K = 10$ as a function of the model parameter α_A for $l = 20°$, $b = 0°$.

This leaves α_r as the principal parameter to be determined by the relevant data. The sensitivity of the model to variations in α_r is illustrated in Fig. A1 for two different lines of sight. As expected, the dependance of the source counts on α_r is most dramatic in the plane. Unfortunately variations in the interstellar extinction will have a significant effect for areas in the plane as well. Clumpiness in the extinction may explain the high source counts at $l = 320$, $b = 0$ (Fig. 3). The dependence of the source counts down to $K = +10$ at $l = 20$, $b = 0$ on α_A, the absorption scale length, is illustrated in Fig. A2. If the observed reddening to the Galactic Centre is anomalously high (e.g. a dark cloud is by chance directly intervening) then a longer scale length may be appropriate. None the less, the gas density does increase interior to the Sun and one would expect the extinction (i.e. dust) to do the same. Note that the sensitivity of the source counts is not as great for variations in α_A as for α_r.

Fig. A3 illustrates the model dependence of the 2.2 μm flux on latitude at $l = 20$. The important feature of Fig. A3 is the rather weak dip in the flux at $b = 0$ due to extinction in the plane. Through large beams ($\lesssim 0.5°$) such as those used to measure the 2.4 μm flux distribution, this dip would not show up and indeed, there is no evidence for such a dip in the observations (Hayakawa *et al.* 1980).

A portion of a typical output from the model is given in Table A1 for $l = 20°$, $b = 0°$ and in Table A2 for $l = 20°$, $b = 10°$ where the entries are in number per square degree brighter

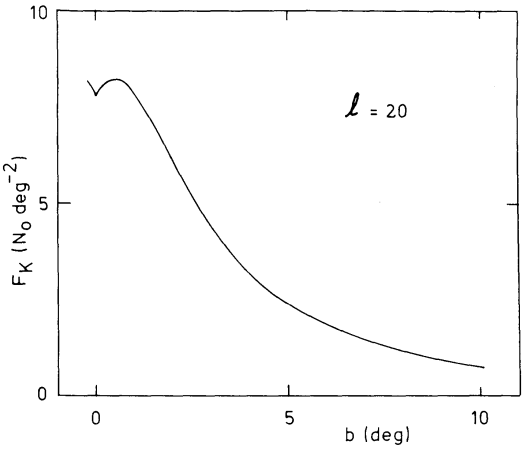

Figure A3. The computed surface brightness at 2.2 μm (in units of the equivalent number of 0.0 mag stars deg^{-2}) for $l = 20°$ as a function of galactic latitude.

Table A1. Sample output: $\lambda = 2.2\,\mu m$, $l = 20°$, $b = 0°$.

SPECTRAL TYPE	TO MAG 3	TO MAG 4	TO MAG 5	TO MAG 6	TO MAG 7	TO MAG 8	TO MAG 9	TO MAG 10	TO MAG 11	TO MAG 12
B0, 1	0.5678E-03	0.2318E-02	0.9596E-02	0.4052E-01	0.1759E+00	0.7873E+00	0.3601E+01	0.1612E+02	0.6502E+02	0.2156E+03
B2, 3	0.3543E-03	0.1427E-02	0.5783E-02	0.2367E-01	0.9832E-01	0.4174E+00	0.1823E+01	0.8211E+01	0.3757E+02	0.1658E+03
B5	0.2121E-03	0.8516E-03	0.3433E-02	0.1394E-01	0.5718E-01	0.2384E+00	0.1017E+01	0.4471E+01	0.2025E+02	0.9248E+02
B8-A0	0.1101E-02	0.4416E-02	0.1774E-01	0.7155E-01	0.2908E+00	0.1195E+01	0.4997E+01	0.2139E+02	0.9442E+02	0.4289E+03
A2-5	0.4123E-03	0.1660E-02	0.6653E-02	0.2671E-01	0.1077E+00	0.4370E+00	0.1793E+01	0.7475E+01	0.3189E+02	0.1402E+03
F0-5	0.7483E-03	0.3033E-02	0.1217E-01	0.4882E-01	0.1964E+00	0.7949E+00	0.3246E+01	0.1344E+02	0.5676E+02	0.2464E+03
F8-G2 V	0.1946E-03	0.8681E-03	0.3556E-02	0.1429E-01	0.5729E-01	0.2300E+00	0.9277E+00	0.3768E+01	0.1548E+02	0.6462E+02
G5 V	0.1344E-03	0.6545E-03	0.2729E-02	0.1101E-01	0.4416E-01	0.1771E+00	0.7129E+00	0.2887E+01	0.1180E+02	0.4894E+02
G8-K3 V	0.1481E-03	0.9313E-03	0.4088E-02	0.1669E-01	0.6707E-01	0.2689E+00	0.1081E+01	0.4365E+01	0.1777E+02	0.7325E+02
K4-5 V	0.6804E-04	0.5904E-03	0.2773E-02	0.1148E-01	0.4628E-01	0.1856E+00	0.7449E+00	0.3003E+01	0.1219E+02	0.4998E+02
M0-1 V	0.1573E-04	0.2906E-03	0.1660E-02	0.7148E-02	0.2906E-01	0.1167E+00	0.4679E+00	0.1882E+01	0.7607E+01	0.3102E+02
M2-3 V	0.1965E-05	0.1078E-03	0.9358E-03	0.4394E-02	0.1820E-01	0.7334E-01	0.2941E+00	0.1181E+01	0.4759E+01	0.1931E+02
M4-5 V	0.6131E-05	0.7652E-04	0.5427E-03	0.2711E-02	0.1158E-01	0.4710E-01	0.1894E+00	0.7611E+00	0.3072E+01	0.1249E+02
F8-G2 III	0.4052E-03	0.1629E-02	0.6572E-02	0.2674E-01	0.1100E+00	0.4607E+00	0.1975E+01	0.8706E+01	0.3921E+02	0.1747E+03
G5 III	0.8465E-03	0.3409E-02	0.1381E-01	0.5649E-01	0.2343E+00	0.9926E+00	0.4319E+01	0.1930E+02	0.8697E+02	0.3774E+03
G8 III	0.4170E-02	0.1679E-01	0.6796E-01	0.2778E+00	0.1151E+01	0.4871E+01	0.2117E+02	0.9465E+02	0.4289E+03	0.1885E+04
K0, 1 III	0.1234E-01	0.4968E-01	0.2011E+00	0.8220E+00	0.3407E+01	0.1441E+02	0.6265E+02	0.2805E+03	0.1275E+04	0.5634E+04
K2, 3 III	0.1784E-01	0.7216E-01	0.2944E+00	0.1217E+01	0.5133E+01	0.2222E+02	0.9910E+02	0.4505E+03	0.2006E+04	0.8146E+04
K4, 5 III	0.1898E-01	0.7790E-01	0.3249E+00	0.1387E+01	0.6094E+01	0.2756E+02	0.1254E+03	0.5419E+03	0.2037E+04	0.6169E+04
M0 III	0.9039E-02	0.3755E-01	0.1593E+00	0.6955E+00	0.3128E+01	0.1427E+02	0.6279E+02	0.2453E+03	0.7827E+03	0.1942E+04
M1 III	0.5837E-02	0.2436E-01	0.1041E+00	0.4580E+00	0.2073E+01	0.9431E+01	0.4058E+02	0.1515E+03	0.4541E+03	0.1053E+04
M2 III	0.9741E-02	0.4097E-01	0.1768E+00	0.7867E+00	0.3583E+01	0.1612E+02	0.6658E+02	0.2313E+03	0.6335E+03	0.1339E+04
M3 III	0.1908E-01	0.8116E-01	0.3553E+00	0.1602E+01	0.7302E+01	0.3191E+02	0.1228E+03	0.3835E+03	0.9298E+03	0.1748E+04
M4 III	0.4560E-01	0.1985E+00	0.8903E+00	0.4062E+01	0.1800E+02	0.7143E+02	0.2333E+03	0.5944E+03	0.1171E+04	0.1831E+04
M5 III	0.1425E+00	0.6337E+00	0.2891E+01	0.1308E+02	0.5445E+02	0.1898E+03	0.5164E+03	0.1074E+04	0.1747E+04	0.2313E+04
M6 III	0.1786E+00	0.8149E+00	0.3686E+01	0.1535E+02	0.5349E+02	0.1455E+03	0.3027E+03	0.4925E+03	0.6518E+03	0.7311E+03
M7 III	0.3557E+00	0.1609E+01	0.6699E+01	0.2335E+02	0.6353E+02	0.1321E+03	0.2150E+03	0.2845E+03	0.3191E+03	0.3265E+03
M8 + III	0.5843E+00	0.2432E+01	0.8478E+01	0.2307E+02	0.4797E+02	0.7805E+02	0.1033E+03	0.1159E+03	0.1185E+03	0.1187E+03
YOUNG OB	0.7716E-02	0.3369E-01	0.1511E+00	0.6782E+00	0.2913E+01	0.1122E+02	0.3687E+02	0.1004E+03	0.2248E+03	0.4153E+03
A-G I-II	0.5681E-01	0.2432E+00	0.9181E+00	0.2816E+01	0.7020E+01	0.1456E+02	0.2571E+02	0.3949E+02	0.5394E+02	0.6680E+02
K-M2 I-II	0.4713E+00	0.1743E+01	0.5394E+01	0.1355E+02	0.2745E+02	0.4543E+02	0.6278E+02	0.7476E+02	0.8024E+02	0.8177E+02
M3-4 I-II	0.1281E+01	0.3578E+01	0.8067E+01	0.1474E+02	0.2221E+02	0.2836E+02	0.3186E+02	0.3312E+02	0.3339E+02	0.3342E+02

1981MNRAS.197..413J

Table A2. Sample output: $\lambda = 2.2\,\mu m$, $l = 20°$, $b = 10°$.

SPECTRAL TYPE	TO MAG 3	TO MAG 4	TO MAG 5	TO MAG 6	TO MAG 7	TO MAG 8	TO MAG 9	TO MAG 10	TO MAG 11	TO MAG 12
B0, 1	0.3024E-03	0.8753E-03	0.2168E-02	0.4364E-02	0.6852E-02	0.8467E-02	0.8967E-02	0.9028E-02	0.9030E-02	0.9030E-02
B2, 3	0.2669E-03	0.9156E-03	0.2898E-02	0.8151E-02	0.1942E-01	0.3718E-01	0.5533E-01	0.6558E-01	0.6824E-01	0.6849E-01
B5	0.1741E-03	0.6247E-03	0.2114E-02	0.6556E-02	0.1791E-01	0.4101E-01	0.7478E-01	0.1058E+00	0.1211E+00	0.1244E+00
B8-A0	0.1020E-02	0.3916E-02	0.1468E-01	0.5315E-01	0.1827E+00	0.5810E+00	0.1648E+01	0.3980E+01	0.7759E+01	0.1176E+02
A2-5	0.3993E-03	0.1578E-02	0.6146E-02	0.2357E-01	0.8845E-01	0.3211E+00	0.1109E+01	0.3550E+01	0.1017E+02	0.2485E+02
F0-5	0.7340E-03	0.2943E-02	0.1161E-01	0.4531E-01	0.1747E+00	0.6610E+00	0.2434E+01	0.8595E+01	0.2853E+02	0.8644E+02
F8-G2 V	0.1935E-03	0.8608E-03	0.3509E-02	0.1400E-01	0.5544E-01	0.2184E+00	0.8554E+00	0.3320E+01	0.1272E+02	0.4781E+02
G5 V	0.1338E-03	0.6505E-03	0.2704E-02	0.1085E-01	0.4315E-01	0.1708E+00	0.6733E+00	0.2641E+01	0.1028E+02	0.3959E+02
G8-K3 V	0.1476E-03	0.9270E-03	0.4061E-02	0.1651E-01	0.6595E-01	0.2619E+00	0.1037E+01	0.4093E+01	0.1609E+02	0.6287E+02
K4-5 V	0.6779E-04	0.5877E-03	0.2754E-02	0.1136E-01	0.4551E-01	0.1808E+00	0.7149E+00	0.2815E+01	0.1102E+02	0.4280E+02
M0-1 V	0.1568E-04	0.2894E-03	0.1650E-02	0.7087E-02	0.2868E-01	0.1143E+00	0.4528E+00	0.1787E+01	0.7018E+01	0.2737E+02
M2-3 V	0.1958E-05	0.1074E-03	0.9314E-03	0.4364E-02	0.1801E-01	0.7213E-01	0.2865E+00	0.1133E+01	0.4462E+01	0.1747E+02
M4-5 V	0.6108E-05	0.7619E-04	0.5397E-03	0.2690E-02	0.1145E-01	0.4625E-01	0.1840E+00	0.7278E+00	0.2864E+01	0.1120E+02
F8-G2 III	0.3982E-03	0.1585E-02	0.6303E-02	0.2506E-01	0.9978E-01	0.3985E+00	0.1602E+01	0.6515E+01	0.2681E+02	0.1091E+03
G5 III	0.8280E-03	0.3294E-02	0.1310E-01	0.5210E-01	0.2077E+00	0.8320E+00	0.3363E+01	0.1378E+02	0.5670E+02	0.2225E+03
G8 III	0.3993E-02	0.1568E-01	0.6113E-01	0.2357E+00	0.8943E+00	0.3316E+01	0.1189E+02	0.4047E+02	0.1270E+03	0.3489E+03
K0, 1 III	0.1170E-01	0.4565E-01	0.1762E+00	0.6689E+00	0.2478E+01	0.8857E+01	0.3002E+02	0.9398E+02	0.2611E+03	0.6088E+03
K2, 3 III	0.1648E-01	0.6371E-01	0.2425E+00	0.9022E+00	0.3244E+01	0.1109E+02	0.3518E+02	0.9970E+02	0.2392E+03	0.4531E+03
K4, 5 III	0.1714E-01	0.6653E-01	0.2553E+00	0.9644E+00	0.3558E+01	0.1262E+02	0.4178E+02	0.1202E+03	0.2592E+03	0.3692E+03
M0 III	0.7831E-02	0.3014E-01	0.1143E+00	0.4242E+00	0.1521E+01	0.5132E+01	0.1538E+02	0.3590E+02	0.5596E+02	0.6258E+02
M1 III	0.4971E-02	0.1907E-01	0.7197E-01	0.2652E+00	0.9391E+00	0.3096E+01	0.8835E+01	0.1877E+02	0.2631E+02	0.2811E+02
M2 III	0.8079E-02	0.3083E-01	0.1155E+00	0.4205E+00	0.1458E+01	0.4619E+01	0.1211E+02	0.2220E+02	0.2742E+02	0.2819E+02
M3 III	0.1519E-01	0.5751E-01	0.2129E+00	0.7604E+00	0.2546E+01	0.7509E+01	0.1699E+02	0.2551E+02	0.2802E+02	0.2822E+02
M4 III	0.3315E-01	0.1234E+00	0.4443E+00	0.1511E+01	0.4600E+01	0.1110E+02	0.1806E+02	0.2065E+02	0.2091E+02	0.2092E+02
M5 III	0.9365E-01	0.3414E+00	0.1187E+01	0.3773E+01	0.9904E+01	0.1762E+02	0.2066E+02	0.2092E+02	0.2092E+02	0.2092E+02
M6 III	0.9622E-01	0.3345E+00	0.1063E+01	0.2791E+01	0.4965E+01	0.5822E+01	0.5895E+01	0.5896E+01	0.5896E+01	0.5896E+01
M7 III	0.1460E+00	0.4642E+00	0.1218E+01	0.2167E+01	0.2541E+01	0.2573E+01	0.2574E+01	0.2574E+01	0.2574E+01	0.2574E+01
M8 + III	0.1685E+00	0.4424E+00	0.7868E+00	0.9227E+00	0.9343E+00	0.9345E+00	0.9345E+00	0.9345E+00	0.9345E+00	0.9345E+00
YOUNG OB	0.1264E-02	0.2576E-02	0.4394E-02	0.6275E-02	0.7676E-02	0.8402E-02	0.8655E-02	0.8713E-02	0.8722E-02	0.8723E-02
A-G I-II	0.3878E-03	0.5012E-03	0.5918E-03	0.6520E-03	0.6848E-03	0.6988E-03	0.7031E-03	0.7038E-03	0.7039E-03	0.7039E-03
K-M2 I-II	0.6396E-03	0.6584E-03	0.6617E-03	0.6621E-03	0.6621E-03	0.6621E-03	0.6621E-03	0.6621E-03	0.6621E-03	0.6621E-03
M3-4 I-II	0.2692E-03	0.2697E-03	0.2697E-03	0.2697E-03	0.2697E-03	0.2697E-03	0.2697E-03	0.2697E-03	0.2697E-03	0.2697E-03

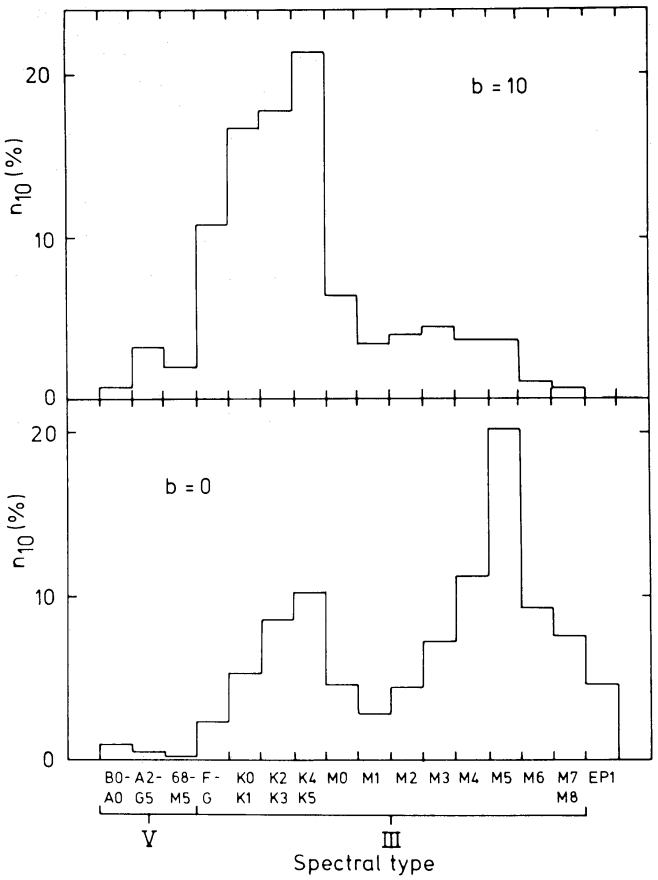

Figure A4. Histogram of the percentage contribution of spectral type classes to the number of stars brighter than $K = +10$ predicted by the model for $l = 20°$. Two different latitudes are shown.

than the K magnitude at the top of each column. The general characteristics of this model output are illustrated in Fig. A4, which is a histogram of the relative contributions of the various spectral types to the stellar field for stars brighter than apparent magnitude $K = +10$. Note that the main sequence and extreme Population I stars (last four rows in Table 2) make up a very small proportion of the field. The field is completely dominated by disc

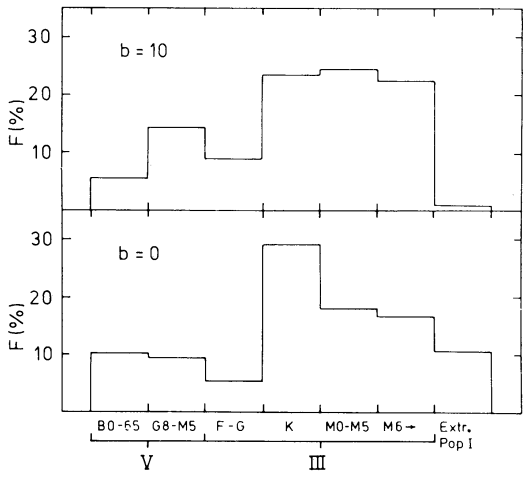

Figure A5. Histogram of the percentage contribution of spectral type classes to the surface brightness at K predicted by the model for $l = 20°$. Two different latitudes are shown.

giants for $K \leqslant 10$. The shift in proportionate numbers from M to K giants for $b = 10^\circ$ is due to the line of sight becoming galaxy bounded for the much brighter M stars. As the magnitude limit is made fainter than $K = 10$, the proportion of main sequence stars increases as giants of ever earlier spectral type (i.e., fainter M_K) become galaxy bounded and no longer add numbers into the field. This can best be seen in Fig. A5, which is a histogram of the relative contributions of the various spectral types to the total integrated flux at $\lambda = 2.2\,\mu$m and $l = 20^\circ$. The large numbers of intrinsically fainter stars adding in at fainter apparent magnitudes make a significant contribution to the flux. Only the extreme Population I stars show a radical difference between $b = 0$ and $b = 10$.

In summary, the model for the near infrared luminosity function developed here behaves in an entirely reasonable manner and does an excellent job of fitting source count data in lines of sight more than 1° out of the plane. The model fit in the plane is not as consistently good, but quite acceptable, and more than adequate for use in determining the expected field confusion in IR searches for OH maser sources. One of us (AR-M) will be making further scans at $2.2\,\mu$m and multicolour IR photometry of the sources for selected directions in the galaxy to further improve the model and to better determine the extinction (reddening) in the galactic plane.